

# Automatic DTM Generation from Three-Line-Scanner (TLS) Images

Armin Gruen, Zhang Li

Institute of Geodesy and Photogrammetry, Swiss Federal Institute of Technology Zurich  
ETH-Hoenggerberg, CH-8093 Zurich, Switzerland  
Tel.: +41-1-633 31 57, Fax: +41-1-633 11 01  
E-mail: <agruen><zhangl>@geod.baug.ethz.ch

Commission III, WG III/2

**KEY WORDS:** Three-Line-Scanner (TLS), Relaxation Matching, Geometrically Constrained Multi-Image and Multi-point Matching, DSM

## ABSTRACT:

This paper presents a matching procedure for automatic DSM generation from the Three-Line-Scanner (TLS) raw images. It can provide dense, precise and reliable results. The proposed method combines matching procedures based on grid point matching and feature point matching. Modified Multiphoto Geometrically Constrained Matching (MPGC) and Geometrically Constrained Multi-point Matching (GCMM) are used to refine the relaxation matching results in order to achieving sub-pixel accuracy on the grid DSM. We match three TLS images and provide the pixel and object coordinates for grid points simultaneously.

In order to compensate the disadvantages of terrain modeling by grid points, an additional feature-point matching procedure is performed. The feature points are extracted by using an interest operator such as Moravec's. Then we activate the modified MPGC, using three TLS images simultaneously, and achieve potentially sub-pixel accuracy.

The sensor model used for the geometric constraints derivation is based on the collinearity equations appended by some trajectory models.

The algorithms proposed in this paper have been applied to different areas with varying textures and terrain types. The accuracy test is based on the comparison between well-distributed semi-automatically measured feature points and the automatic extracted DSMs, and on visual inspection of the results.

## 1. Introduction

With the advent of large format digital aerial cameras an increased need for reliable automated image analysis functions emerges. The three-line-scanner concept provides for triple overlap in strip direction for every image point and as such basically for fairly good reliability characteristics. In addition, the basic capabilities of image matching techniques have so far not been fully utilized yet. This contribution aims at combining the new three-line-scanner sensor model with some novel image matching approaches, as multi-image and multi-point matching. As to the sensor we refer to the TLS system, developed by Starlabo Corporation, Tokyo. Our matching goal is DSM extraction.

The TLS sensor model is based on the collinearity equation and expresses the relationship between the pixel and object coordinates. This sensor model is used for the recovery of the exterior orientation parameters for each scan line of the TLS images by a photogrammetric bundle adjustment, and for the derivation of the geometric constraints in our modified Multiphoto Geometrically Constrained (MPGC) matching and Geometrically Constrained Multi-point Matching (GCMM).

This paper presents a matching approach for automatic DSM generation from the TLS raw images. It can provide dense, precise and reliable results. The proposed method is a combined matching procedure, which is based on both grid point matching and features point matching. After image pyramid generation and the extraction of approximations by using a simple feature point matching on the highest level of the image pyramid, grid point matching based on the relaxation technique is performed on a TLS stereo pair which can be any combination of two of the three TLS images. The important aspect of this relaxation matching that differs from other area-based single point matching is its compatible coefficient function and its smoothness constraint satisfaction procedure. With the smoothness constraint, poor texture areas can be bridged assuming the terrain surface varies smoothly over the imaging

area. Modified MPGC and GCMM procedures are used to refine the relaxation matching results in order to achieve sub-pixel accuracy. Both can be used to match three TLS images and provide the pixel and object coordinates for object points simultaneously.

The algorithms proposed in this paper have been applied to different areas with varying textures and terrain types. The accuracy testing is based on the comparison of well-distributed semi-automatically measured feature points to the automatically extracted DSMs and on visual inspection of the DSMs.

## 2. The TLS System

The TLS (Three-Line-Scanner) system is a new airborne digital sensor, developed by Starlabo Corporation, Tokyo. It utilizes the three-line-scanner principle to capture digital image triplets in along-strip mode. The imaging system contains three parallel one-dimensional CCD focal plane arrays, with 10200 pixels of 7 $\mu$ m each (see Figure 1). The TLS system produces seamless high-resolution images (5 - 10 cm footprint on the ground) with three viewing directions (forward, nadir and backward). In order to get highly precise attitude data and high quality raw image data from an aerial platform, a high quality stabilizer is used for the camera and outputs attitude data at 500 Hz. A Trimble MS750 serves as Rover GPS and collects L1/L2 kinematic data at 5 Hz and another Trimble MS750 serves as Base GPS on the ground.

For the TLS sensor and imaging parameters see Table 1.

The image data collected by the TLS imaging system is only useful under the condition that the geometric relationship between pixels and their corresponding ground coordinates, i.e. the sensor model is known. Thus, the sensor modeling is the most important problem to be solved firstly.

Unlike with frame-based photography, the three-line geometry is characterized by nearly parallel projection in the flight direction and perspective projection perpendicular to the flight direction. Our sensor model for the TLS images is based on the

collinearity equations and uses different forms of trajectory models. This sensor model is used for the improvement of the measured exterior orientation parameters for each scan line of TLS images by a modified photogrammetric bundle adjustment, and for the derivation of the geometric constraints in our modified MPGC and GCOMM procedures. More details on our TLS sensor model can be found in Gruen and Zhang, 2002.

Table 1: TLS sensor and imaging parameters

focal length	60.0 mm
number of pixels per array	10200
pixel size	7 $\mu\text{m}$
number of CCD focal plane arrays	3
stereo view angle	21/42 degree*
Field of view	61.5 degree
instantaneous field of view	0.0065 degree
scan line frequency	500 HZ

\* forward-nadir/forward-backward stereo view angle

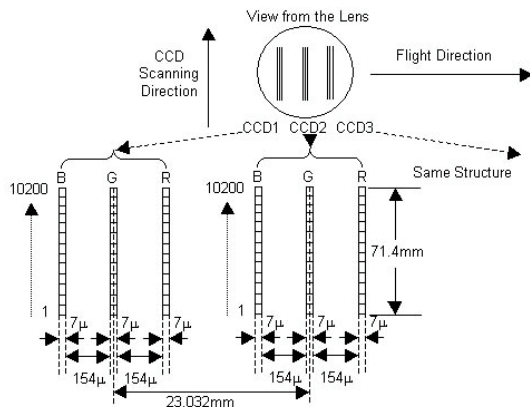


Figure 1: TLS CCD sensor configuration

### 3. Matching Considerations

The automatic generation of DTMs has gained much attention in the past years. A wide variety of approaches have been developed, and automatic DTM generation packages are in the meanwhile commercially available on several digital photogrammetric workstations. Although the algorithms and the matching strategies used may differ from each other, the accuracy performance and the problems encountered are very similar in the major systems and the performance of commercial image matchers does by far not live up to the standards set by manual measurements (Gruen et al., 2000). The main problems in DTM generation are encountered with

- (a) Little or no texture
- (b) Distinct object discontinuities
- (c) Local object patch is no planar face in sufficient approximation
- (d) Repetitive objects
- (e) Occlusions
- (f) Moving objects, incl. shadows
- (g) Multi-layered and transparent objects
- (h) Radiometric artifacts, like specular reflections and others
- (i) Reduction from DSM to DTM

The degree to which these problems will influence the matching results is image scale dependent. A DTM derived from 10m pixelsize SPOT images will be relatively better than one derived from 10cm pixelsize TLS images.

Area-based, feature-based and relational matching have both advantages and disadvantages with respect to these problems. The key to successful matching is an appropriate matching strategy, making use of all available and explicit knowledge concerning sensor model, network structure and image content.

But even then the lack in image understanding capability will lead to problems, whose relevance must be judged by the project specifications.

This paper presents a matching procedure for automatic DSM generation from the TLS raw images that can provide dense, precise and reliable results and addresses the problems (a)-(f) mentioned above. The proposed method is a combined matching procedure, which is based on both grid point matching and feature point matching. The presented results reflect an intermediate stage of development. We are fully aware that more refinements are needed before automated matching can be considered a highly reliable procedure.

Figure 2 shows the strategy of our matching approach. We use the raw TLS images and the given or previously triangulated orientation elements. After production of the image pyramids we extract on the upper pyramid level a first approximation DSM by a geometrically constrained feature point matching based on cross-correlation. Next we run a grid point based relaxation matching scheme through all pyramid levels. We select the grid width to 11 pixels on all levels. The matching candidates are obtained by a cross-correlation-based geometrically constrained matching, as described in chapter 4.1. At each level we obtain a refined DSM, which in turn is used in the subsequent pyramid level for the candidate search. The important aspect of this relaxation method is its compatible coefficient function and its smoothness constraint satisfaction scheme. The smoothness constraint links the matching results of the neighbouring grid points to each other and achieves global consistency in the matching. The weight of the smoothness constraint is related to the image texture information and provides the possibility of controlling the continuity of the terrain surface. With the smoothness constraint, image areas with little or no texture information can be bridged by assuming that the terrain surface varies smoothly over the area.

Next we can either activate a modified Multiphoto Geometrically Constrained Matcher (MPGC) or a Geometrically Constrained Multi-point Matcher (GCOMM). Both may be considered as refinements of the relaxation matching results and are used in order to achieve sub-pixel accuracy.

The modified multi-point matching with geometric constraints is characterized by its smoothness constraints in the 2D parallax domain. By including geometrical constraints, it can be used to match three TLS images simultaneously and provide the pixel and object coordinates for each nadir image grid point simultaneously.

In order to compensate the disadvantages of terrain modeling by grid points, a feature point matching procedure which exploits the modified MPGC has also been implemented. In this procedure, the feature points are extracted by using some interest operator such as Moravec's. The relaxation matching results provide quite good approximations.

The weighted geometric constraints in the modified MPGC and GCOMM forces the matching to search for a conjugate point only along the epipolar curves. This reduction of the search space from 2D to 1D increases the success rate and reliability of the feature point matching results. Moreover, the geometric constraints derived from the TLS sensor model link the grid matching results of the three TLS images and have the ability to solve the problem of repetitive objects, occlusions and moving objects in image matching.

According to Hsia and Newton, 1999, using a combination of feature points, grid points and filling back points can give encouraging results for DTM production. The results of using three different TLS data sets from Japan (city, sub-urban and mountainous area) will be reported in this paper.

#### 4. The Matching Approach

In our application of automatic DSM generation from TLS imagery, a combination of algorithms for grid point matching and feature point matching is used. Image pyramids are incorporated into the matching strategy. An image matching algorithm, which has the ability to bridge over the poor texture areas and preserve the terrain features at high accuracy, by using the TLS raw images, was developed. The work-flow of our combined matching approach is shown in Figure 2.

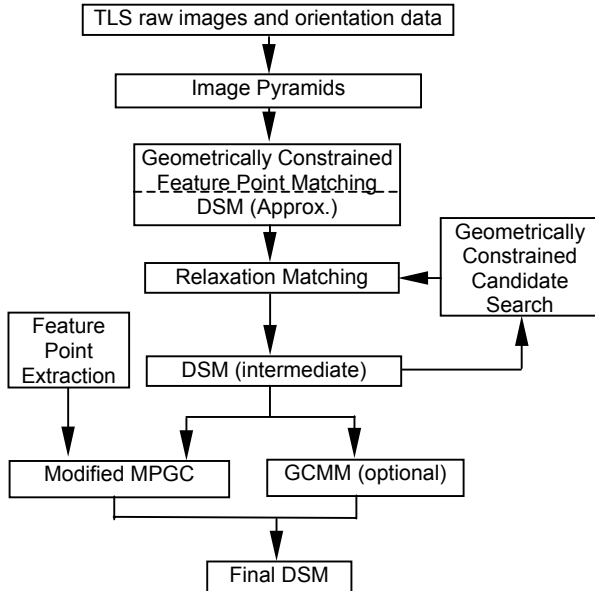


Figure 2: Work-flow of our combined image matching

#### 4.1 Input Data and Derivation of Approximations

The input data includes the TLS strip which normally consists of three images of the forward, nadir and backward view CCD arrays, and information about their interior and exterior orientation parameters (for details see Gruen and Zhang, 2002). Raw images from most other line-scanner digital sensors need a special rectification process in order to eliminate distortions caused by high frequency positional and attitude variations of the camera during the flight. In this rectification process, each scan-line of the raw image data is projected to a planar surface defined by a horizontal plane at the mean terrain height. Because of unknown object model at this point the rectified images have no correct geometry and the results of this process are only quasi-epipolar images. In the TLS system, a high quality stabilizer is used in image acquisition, so the raw image data can be directly used for image matching.

The image pyramid starts from the original TLS image. Each pyramid level is generated by multiplying a generation kernel and reduces the resolution by factor 3. The pyramid level number is a pre-defined value which is either a user input or can be determined according to the height range of the imaging area.

The approximations for the following matching procedures are extracted by geometrically constrained feature point matching, which exploits the orientations of the TLS (see Figure 3). Feature point extraction by using the Moravec interest operator is performed on the highest level of the image pyramid in the nadir view TLS image. Given a feature point in the nadir image, an image ray that connects the instant perspective center and this image point can be determined. Given a height approximation  $Z_0$  and a height interval  $\Delta Z$ , the coordinates of three object points  $(X_u, Y_u, Z_0 + \Delta Z)$ ,  $(X_0, Y_0, Z_0)$  and  $(X_l, Y_l, Z_0 - \Delta Z)$  can be computed by using the pixel coordinates and orientation elements. The height approximation  $Z_0$  and the value

$\Delta Z$  can be derived from the user input (the maximum, minimum and the average terrain height of the imaging area). By projecting these three object points back to the forward and backward view images, search windows can be determined. These windows are assumed to be rectangular for a small region in first approximation. Their width is  $\pm 5$  to 11 pixels depending on the level of the pyramid. The matches in the search images are derived by cross-correlation technique, and they are accepted if their correlation coefficient lies above a certain user-defined threshold. We choose this threshold value as 0.9. As a result, for each feature point on the nadir view TLS image a conjugate image point triplet can be obtained. By using forward intersection some blunders can be detected. The matching result is used to interpolate the approximate values for the following relaxation matching on the highest level of the image pyramid.

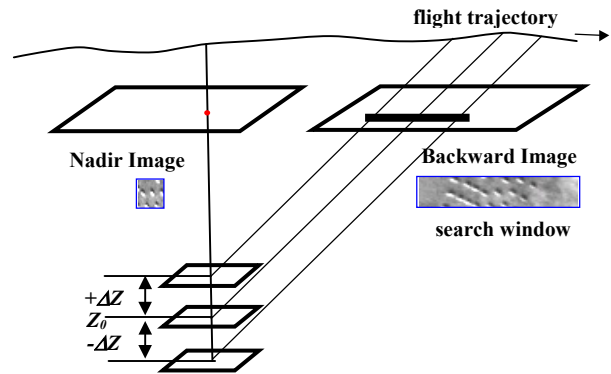


Figure 3: The determination of the search window

#### 4.2 Grid Point Matching based on Relaxation

The matching procedure can be treated as a labeling problem and solved by relaxation technique. That is, we regard the template image (for example, the nadir view image) as the model and another image as the scene, and then use the feature points in the model as a set of labels to label the feature points extracted from the scene. Relaxation is one of the efficient methods to solve the labeling problem. The work of Hancock and Kittler, 1990 that uses Bayesian probability theory has provided a theoretical framework and rigorous basis for the relaxation method.

The important aspect of the relaxation matching algorithm that distinguishes it from the single point matching is its compatible coefficient function and its smoothness constraint satisfaction scheme (Baltasvias, 1991; Zhang et al, 1992). This is most important for areas with homogeneous or only little texture. In such areas, the single point matching is unable to match images because of the lack of information. With the smoothness constraint, such areas can be bridged over, assuming that the terrain surface varies smoothly over the area.

Firstly, the points are selected in form of a regular grid in the template image (nadir view image). Given a grid point in the template image, a search window can be determined (see Figure 3). The correct match of this point should lie in this search window. However, due to repetitive texture or poor texture information, there could be several candidate matches appearing in the search window. These candidate matches are located along the epipolar curve. They can be derived by traditional cross-correlation technique, and the candidate matches are selected if their correlation coefficient lies above a certain user-defined threshold (we choose this threshold value as 0.7). The approximations can be derived from the matching results of the previous pyramid level.

Let  $I_i$  be one of the grid points on the template image and  $I_j$  ( $j=1, \dots, m$ ) its candidate matches on the search image.  $P(i, j)$  is the probability of match  $I_i \leftarrow I_j$ . Moreover, let  $I_k$  be one of the

points located in the neighborhood of point  $I_i$  and  $I_l$  ( $l=1, \dots, m$ ) are its corresponding candidate matches.

In order to link the matching results of the neighboring grid points to each other, we define the following compatible coefficient function  $C(i, j; k, l)$  which quantifies the compatibility between the match  $I_i \leftarrow I_j$  and a neighboring match  $I_k \leftarrow I_l$ :

$$C(i, j; k, l) = \frac{T}{\exp(\Delta p^2 / \beta)} \quad (1)$$

$$\text{where } \Delta p = (x_j - x_i) - (x_l - x_k)$$

In equation (1),  $\Delta p$  expresses the difference of the x-parallaxes in point  $I_i$  and its neighboring point  $I_k$ . The bigger the  $\Delta p$ , the smaller the compatibility. This corresponds to a smoothness constraint on the image matching results.  $T$  is a value quantified by the texture information and it is defined as inversely proportional to the minimum of four gray value variances (horizontal, vertical, and two main diagonals) at the image window around the point  $I_i$ . Normally, if one point is located in rich texture areas or at linear features, this value is small. This value can be treated as the weight of the smoothness constraint and it provides the possibility to control the continuity of the terrain surface.  $\beta$  is a constant value and is set to 400 experimentally.

In the relaxation scheme, the so-called global consistency of matching can be achieved by an iterative scheme where the probabilities  $P(i, j)$  are updated by the following rule:

$$P^{(n+1)}(i, j) = \frac{P^{(n)}(i, j) Q^{(n)}(i, j)}{\sum_{s=1}^m P^{(n)}(i, s) Q^{(n)}(i, s)} \quad (2)$$

$$\text{where } Q^{(n)}(i, j) = \prod_{I_k \in \Omega(I_i)} \sum_{l=1}^m P^{(n)}(k, l) C(i, j; k, l)$$

$C(i, j; k, l)$  is the compatible coefficient function defined as above,  $\Omega(I_i)$  is the neighbourhood of point  $I_i$  (can be its 8 or 24 neighboring points), and  $n$  is the iteration number. The quantity  $Q^{(n)}(i, j)$  expresses the support the match  $I_i \leftarrow I_j$  receives at the  $n^{\text{th}}$  iteration step from the matches  $I_k \leftarrow I_l$  in its neighbourhood  $\Omega(I_i)$ . The iteration scheme can be initialized by assigning the normalized correlation coefficient to  $P^{(0)}(i, j)$  and, ideally the process will terminate when an unambiguous match result is reached, that is when each point  $I_i$  is matched with one candidate with probability 1, the probabilities for all other candidate matches for this point being zero. In practice we terminate the process if any one of the following 2 conditions holds:

- For each grid point  $I_i$ , one of the match probabilities  $P(i, j)$  ( $j=1, \dots, m$ ) exceeds  $1-\varepsilon$ , where  $\varepsilon \ll 1$  (for example, we set the value of  $\varepsilon$  to 0.1).

- The pre-defined number of iterations has been reached.

When the iterative procedure is terminated, the match which gains the highest probability  $P(i, j)$  ( $j=1, \dots, m$ ) is selected as the actual match.

This method is performed by using the stereo pairs, which can be a combination of the forward and nadir view or the nadir and backward view TLS images. For speeding up the processing, reduction of the search range and the gain of higher reliability, a multi-resolution data structure, i.e. the image pyramid is used. The matching scheme is performed as follows:

- Construct the image pyramid with a pre-defined number of levels
- Perform the standard relaxation matching with the initial values on the highest level of the pyramid
- Transfer the results from the previous pyramid level to the current level as the starting initial values

- Perform the standard relaxation matching on the current pyramid level using the initial values obtained in step (3)
- Check if the matching has reached the finest pyramid level. If it has not, advance the matching by one level and go to step (4). If it has reached the finest level, terminate the matching procedure

The advantage of this method is that it can achieve reasonable matching results even in areas of little or no texture. Its disadvantage is that the matching results only have pixel-level accuracy. The relaxation matching results are further refined by the following modified MPGC and GCOMM procedures. Another disadvantage is its failure to match all 3 TLS images simultaneously. Also, the grid matching results cannot express the terrain precisely in case the terrain is steep and rough. Under these conditions, some well-distributed feature points can compensate for this disadvantage.

### 4.3 Modified Geometrically Constrained Multi-Point Matching

A multi-point matching algorithm was suggested by Rosenholm, 1986 and further developed by Rauhala, 1988 and Li, 1989. Gruen, 1985b also proposed a conceptually similar method as multi-patch matching. The standard multi-point matching algorithm is image-based and uses the simultaneous computation of parallaxes in grid points which are connected with bilinear finite elements describing the parallax differences. Additional weighted continuity constraints on parallaxes are used to strengthen the connections between the grid points. The critical points of multi-point matching are the selection of the number of nodes in the grid mesh, the size of the image patch and the weight of the smoothness constraints.

Our modified algorithm is an extension of the standard multi-point matching, using parallaxes in two directions and integrating the geometric constraints derived from the TLS sensor model. It can be used to match grid points on three TLS raw images simultaneously and provide the pixel and object coordinates simultaneously.

In the case of matching of TLS images the geometric constraints are derived from the collinearity equations by Taylor expansion and result in

$$\begin{aligned} v_x &= -\frac{\partial I_x}{\partial v} \Delta v + \frac{\partial E_x}{\partial u} \Delta u + \frac{\partial E_x}{\partial X} \Delta X + \frac{\partial E_x}{\partial Y} \Delta Y + \frac{\partial E_x}{\partial Z} \Delta Z + (I_x^0 - E_x^0) \\ v_y &= -\frac{\partial I_y}{\partial v} \Delta v + \frac{\partial E_y}{\partial u} \Delta u + \frac{\partial E_y}{\partial X} \Delta X + \frac{\partial E_y}{\partial Y} \Delta Y + \frac{\partial E_y}{\partial Z} \Delta Z + (I_y^0 - E_y^0) \end{aligned} \quad (3)$$

These two equations can be treated as weighted observation equations in GCOMM. ( $\Delta u$ ,  $\Delta v$ ) are the unknown x-shift and y-shift in pixels, which relate the common unknowns (parallax in x and y direction), appearing in the gray level observations of the standard 2D multi-point matching through the following equations:

$$\begin{aligned} x_s - x_t &= p_x \\ y_s - y_t &= p_y \end{aligned} \quad (4)$$

( $x_t$ ,  $y_t$ ) and ( $x_s$ ,  $y_s$ ) are pixel coordinates of the template and search image respectively,  $p_x$  and  $p_y$  are parallaxes in x and y direction.

The weighted geometric constraints link the parallaxes in three TLS images and in principle, they force the matches for each grid point to move along their respective epipolar curves.

One important issue is how to construct these weighted observation equations, because the computation of the derivatives in equation (3) needs the functions of the six exterior orientation elements with respect to the pixel coordinate  $u$ . Due to the small pull-in range of multi-point matching, we use the grid matching results as initial values. So the correct match can be achieved in a very small image search window, that means we can treat the exterior orientation values as quadratic

polynomials of the pixel coordinate  $u$  by fitting them just using the local segment of the flight trajectory data.

In our implementation, the whole image is covered by overlapping grid meshes of size  $11 \times 11$  nodes. The size of the image patch is  $7 \times 7$  or  $9 \times 9$  pixels. The weight of the smoothness constraints is:

$$w = \lambda / Tex(i) \quad (5)$$

$Tex(i)$  is the minimum of four gray value variances (horizontal, vertical, and two main diagonals) in the image window around the grid point  $i$ .  $\lambda$  is a constant value. To speed up the convergence, stabilize the solution and achieve global consistency,  $\lambda$  in equation (5) starts with a large value and then decreases to permit more precise localization.

However, the very slow convergence rate (normally 20 - 70 iterations are needed for convergence) and the high computation costs (for a  $11 \times 11$  grid mesh, there are  $11 \times 11 \times 2$  unknowns for parallaxes and  $11 \times 11 \times 3$  unknowns for object space coordinates) are the main obstacles for its application. The GCMM is an option in our combined matching approach. In practice, we use the following modified MPGC to refine the matching result of the grid points which have high  $Tex(i)$  values.

#### 4.4 Feature Point Matching based on the Modified MPGC

MPGC was developed by Gruen, 1985a and is described in detail in Baltasvias, 1991. It combines least squares matching and geometric constraints formulated either in image or in object space. The collinearity constraints lead to a 1D search space along epipolar lines, thus to an increase of success rate, precision and reliability, and permit a simultaneous determination of pixel and object coordinates. Any number of images (more than two) can be used simultaneously. The achieved accuracy is in the sub-pixel range. The algorithm also provides criteria for the detection of observation errors and blunders, and the adaptation of the matching parameters to the image and scene content.

The geometric constraints have the same form as equation (3). It can be treated as weighted observation equations in MPGC with  $(\Delta u, \Delta v)$  as the unknown x-shift and y-shift in pixels. For the computation of the derivatives we treat the exterior orientation values as quadratic polynomials of the pixel coordinate  $u$  by fitting them using the local segment of the flight trajectory data. Weighted geometric constraints force the matching to search for a conjugate point only along a small band around the epipolar curve. If the initial match of the point in the search images does not lie on this epipolar curve, it jumps onto this curve at the first iteration of MPGC. Figure 4 shows an example.

The grid point matching results of relaxation between the stereo pairs of the forward-nadir and nadir-backward image combination provide quite good approximations for the MPGC procedure and increase the convergence rate. In our implementation, the adjustment starts only with the two shift parameters and after the first iteration all affine transformation parameters are used. Also, at the first two iterations, the weight value for geometric constraints takes a large value in order to speed up the convergence and then it decreases to consider residual errors in the orientations.

In this procedure, the feature points are extracted by using some interest operator such as Moravec's. We perform the modified MPGC by using three TLS images simultaneously. The pixel and object coordinates for each feature point can be obtained simultaneously.

The advantage of this method is that the matching results have sub-pixel accuracy and these feature points can express the terrain more precisely. The disadvantages are its high computation costs, and in poor texture areas, the height information can be lost as a result of failure of MPGC matching.

This modified MPGC links the pixel and object coordinates through the geometric constraints. It can be further used for model-based matching, which integrates some other types of constraints in object space (Gruen, 1985b) and can also be utilized for semi-automatic or automatic man-made object extraction.

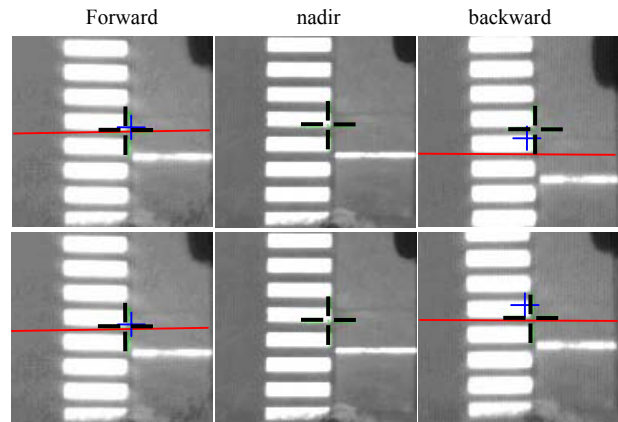


Figure 4: MPGC matching without (above) and with (below) geometric constraints. The line is the corresponding epipolar curve. The small crosses are the initial positions and the big crosses are the final positions.

## 5. Experimental Results

In our experiments, three TLS data sets are used to evaluate the combined matching approach (see Table 2).

Table 2: Test TLS image data sets

Imaging area	Image Scale & Footprint	Descriptions
GSI	1:8000; 5.6 cm	city and sub-urban area with many man-made objects and poor texture areas
DOKEN	1:8000; 5.6 cm	sub-urban area with large areas of poor texture
KOBOTOKE	1:7500; 5.0 cm	mountain area with large areas of forest

For the determination of the position and the attitude values for each image scan-line, a photogrammetric triangulation procedure which models the flight trajectory with piecewise polynomials is performed with the help of the signalized control points. The tie points are extracted using semi-automatic least squares matching. As a result of triangulation, 2.7 - 4.7 cm and 5.1 - 7.8 cm absolute accuracy in planimetry and height respectively are obtained.

The aim of this test is to evaluate the performance of our combined image matching approach. The following 3 versions are executed:

**G\_Rex**: grid point matching based on relaxation

**G\_Rex+GCMM**: refined grid point matching of relaxation by GCMM.

**G\_Rex+F\_MPGC**: combination of relaxation matching refined by modified MPGC and feature point matching based on MPGC.

The aim of using these 3 different versions is to compare the performance of different combinations. The results are shown in Figures 5 - 7.

Matching results of an image window that covers a more undulating terrain with rich textures are shown in Figure 5. Here the version G\_Rex+GCMM and the version G\_Rex+F\_MPGC get similar results. This situation can be explained by the fact

that the rich texture information induces small weight values for smoothness constraints used in GCMM. Small weight values mean that the neighborhood constraints are deactivated such that the matching results are equivalent to the MPGC results.

Figure 6 shows the results of an image window that covers a city area. Version G\_Rex+F\_MP GC gains the best results except some blunders, caused by multiple solutions in direction of the epipolar curve (see region marked "blunders"). If these blunders can be detected, satisfactory DSM results can be achieved by using our matching approach even in city areas, which contain homogeneous texture areas and discontinuities as well.

While the previous analysis of results was based on visual inspection only, we now present a quantitative accuracy test using measured DSM reference points.

The next example shows the KOBOTOKE area (see Figure 8). The final DSM was generated for the entire three-ray area, which covers approximately  $32\,000 \times 10\,200$  pixels (about  $1600 \times 501\text{ m}^2$ ), the height range is 181 - 370 m. The approach starts with the grid point matching based on relaxation. The grid point matching is performed on image pairs. The patch size is  $15 \times 15$  pixels and the grid interval is also  $15 \times 15$  pixels. This step results in about 1 301 586 points for each stereo pair. Then the relaxation matching results are refined by the modified MPGC procedure. The patch size for MPGC is  $21 \times 21$  pixels. At this stage, 247 882 grid points are rejected by the modified MPGC procedure. Most of these points are located in areas with homogeneous texture or low image contrast like forest areas where the accuracy and reliability of the matching results is limited. However, these grid points are kept in order to preserve the completeness of DSM, but they are marked by low matching reliability. For the remaining 1 053 704 grid points, standard deviations of 0.04 - 0.17 pixels in x and y direction, 0.03 - 0.07 m and 0.04 - 0.11 m in object coordinates X-Y and Z are obtained. The feature point matching based on modified MPGC results in 76 935 points with similar accuracy for refined grid point matching results. For accuracy assessment a 0.5 m grid interval DTM was generated from these grid and feature points. The area for the accuracy test is an open area (see Figures 7 and 8), with some terrain discontinuities and little disturbances of man-made objects and trees. We use 118 points measured semi-automatically as check points and the comparison leads to the following values:

Minimum difference:	-0.44 m
Maximum difference:	0.40 m
Mean difference:	0.01 m
RMS Error:	0.15 m

The height accuracy of 0.15 m is worse than the theoretical values (0.04 - 0.11 m) predict. This is to be expected because there are always some artifacts disturbing the proper matching. Also, the reference values are not free of errors, because they are derived from the same image material.

## 6. Conclusions

In cooperation with Starlabo Corporation, Tokyo we are developing a suite of new methods and software for the processing of Three-Line-Scanner (TLS) imagery. In this paper we have reported about our current matching approaches for fully automated DSM generation. The methods and results are of preliminary nature and will be refined in the months to come. We have developed a matching strategy combining grid point approaches (relaxation matching and Geometrically Constrained Multi-point Matching (GCMM)) with neighborhood constraints between the patches and geometrical constraints, with Geometrically Constrained Multi-photo Matching, utilizing feature points. The geometrical constraints are derived from the specific TLS sensor model, which has been published in Gruen

and Zhang, 2002. This strategy allows us to bridge areas with little or no texture and at the same time maintain the important contribution of object/image edges.

As evidenced by a visual inspection of the results we can reproduce small geomorphological features. The results from the quantitative accuracy test ( $RMSE_Z = 0.15\text{ m}$ ) do not match the theoretical expectations ( $\sigma_Z = 0.04 - 0.11\text{ m}$ ) yet, but the presented concept shows great potential for future refinements. A major problem is the control of some small blunders, which still infest the results, despite the simultaneous matching of 3 images.

Another current activity is the derivation of 3D city models with semi-automated matching techniques.

## Acknowledgment

The authors would like to thank Starlabo Corporation, Tokyo for their project support and provision of the test TLS image data sets.

## References

- Baltsavias, E. P., 1991, Multiphoto Geometrically Constrained Matching. Dissertation, IGP, ETH Zürich, Mitteilungen No. 49, 221 pages.
- Gruen, A., 1985a, Adaptive Least Squares Correlation: A powerful Image Matching Technique. South Africa Journal of Photogrammetry, Remote Sensing and Cartography, 14 (3), pp. 175-187.
- Gruen, A., 1985b, Adaptive Kleinste Quadrate Korrelation und Geometrische Zusatzinformationen. Vermessung, Photogrammetrie, Kulturtechnik, 9/85, pp. 309-312.
- Gruen, A., Bär, S., Bühner, Th., 2000: DTMs Derived Automatically From DIPS - Where Do We Stand? Geoinformatics, Vol.3, No.5, July/August, pp. 36-39.
- Gruen, A., Baltsavias, E. P., 1988, Geometrically Constrained Multiphoto Matching. Photogrammetric Engineering and Remote Sensing, Vol. 54, No. 5, pp. 633-641.
- Gruen, A., Zhang, L., 2002. Sensor Modelling for Aerial Mobile Mapping with Three-Line-Scanner (TLS) Imagery. ISPRS Commission II Symposium on Integrated System for Spatial Data Production, Xi'an, P. R. China, August 20 - 23, (submitted for publication).
- Hancock, E. R., Kittler, J., 1990, Discrete relaxation. Pattern Recognition, Vol. 23 pp. 711-733.
- Hsia, J. S., Newton, I., 1999. A Method for the Automated Production of Digital Terrain Models Using a Combination of Feature Points, Grid Points and Filling Back Points. Photogrammetric Engineering and Remote Sensing, Vol 65, June, pp. 713-719.
- Hsia, J. S., 2001, A Research on the Method of Simultaneity Least Squares Multi-Point Matching for producing Digital Terrain Models. In: 22<sup>nd</sup> Asian Conference on Remote Sensing, 5-9 Nov., Singapore.
- Li, M. X., 1989, Hierarchical Multi-point Matching with Simultaneous Detection and Location of Breaklines. Dissertation, The Royal Institute of Technology Department of Photogrammetry, Stockholm, 177 pages.
- Rosenholm, D., 1987, Multi-point Matching using Least-squares Technique for Evaluation of Three-dimensional Models. Photogrammetric Engineering and Remote Sensing, Vol 53, June, pp. 621-626.

Rauhala, U A., 1988, Compiler Positioning System: An Array Algebra Formulation of Digital Photogrammetry. International Archives of Photogrammetry and Remote Sensing, Vol. 27/B9, pp. 151-161.

Zhang, Z., Zhang, J., Wu, X., Zhang, H., 1992, Global Image Matching with Relaxation Method. Proceedings of the International Colloquium on Photogrammetry, Remote Sensing and Geographic Information Systems, 11-14 May, Wuhan, China, pp. 175-188.

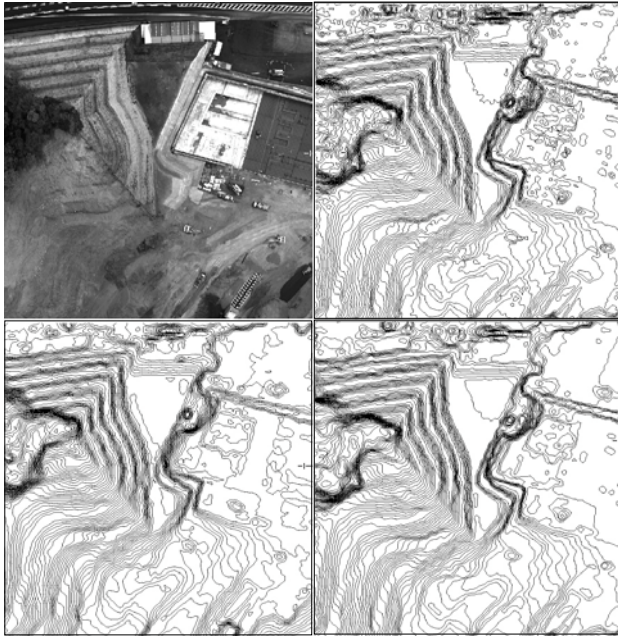


Figure 5: KOBOTOKE matching results; top-left: image window that covers an undulating terrain with rich texture; top-right: contours derived from the G\_Rex matching results; bottom-left: result from G\_Rex+GCMM; bottom-right: result from G\_Rex+F\_MPGC; contour interval: 0.5 m

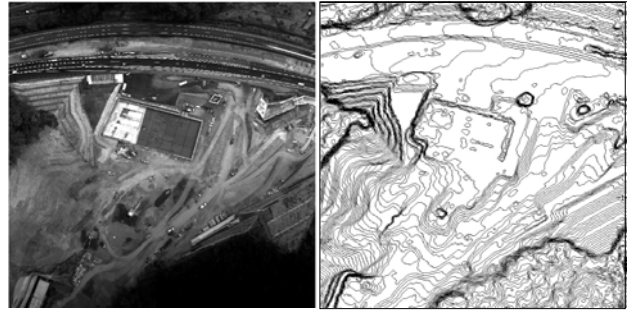


Figure 7: Image window with the area for the accuracy test KOBOTOKE project; left: image; right: contours derived from the G\_Rex+F\_MPGC matching; contour interval: 0.5 m

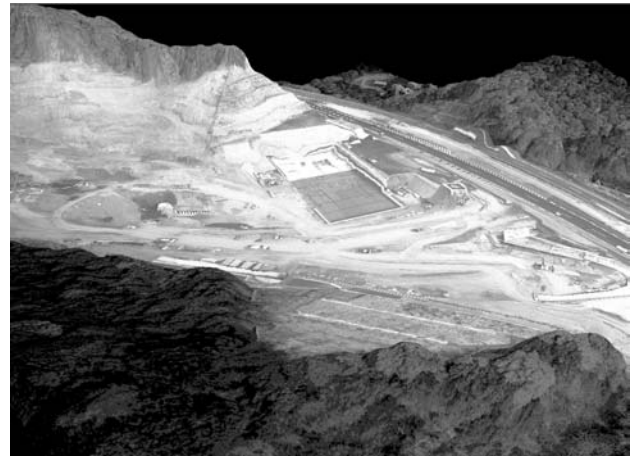


Figure 8: 3D visualization of the KOBOTOKE accuracy test area

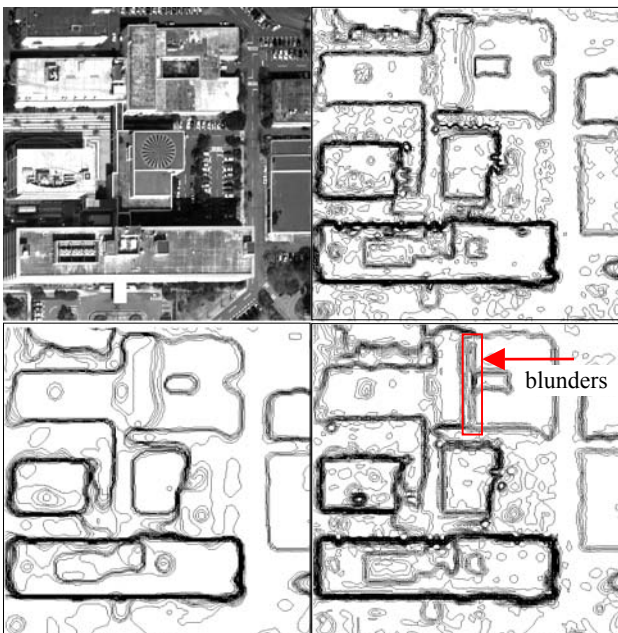


Figure 6: GSI matching results; top-left: image window that covers a city area with rich texture; top-right: contours derived from the G\_Rex matching results; bottom-left: result from G\_Rex+GCMM; bottom-right: result from G\_Rex+F\_MPGC; contour interval: 0.5 m